DOI: 10.7860/JCDR/2024/68552.18938

Case Series

Radiology Section

Magnetic Resonance Imaging of Spinal Bone Marrow Signal Alterations with Emphasis on Pattern Recognition: A Case Series

CHANDRASEKHAR PATIL[1], BHARATH SHEKARAPA GADAGOLI[2], NAINI MANENDER REDDY[3], SREE SREYA CHINNAPOLLA[4], PRASHANTH KUMAR[5]

ABSTRACT

Magnetic Resonance Imaging (MRI) is the most sensitive imaging modality available to detect bone marrow oedema. Different pathological conditions of the spine exhibit distinct and specific bone marrow oedema patterns or signal characteristics. Understanding these patterns for various types of bone marrow oedema in the spine, such as degenerative and pathological conditions, helps to prevent unnecessary investigations and further work-up. In this article, authors detail the specific imaging characteristics of benign versus malignant or pathological fractures, tuberculosis and non tubercular infections of the spine, as well as the imaging appearance of multiple myeloma, among others. Therefore, this article mainly emphasises the approach to bone marrow oedema detected in the spine, aiding in reaching the correct diagnosis and guiding proper management.

Keywords: Metastasis, Multiple myeloma, Spondylodisctis

INTRODUCTION

Back pain is the most common presenting symptom in most spinal conditions, and MRI is an effective diagnostic tool for evaluating back pain. MRI is highly sensitive in detecting early marrow oedema long before morphological changes occur in bone, and it is radiation-free. Another primary imaging modality for evaluation of back pain is X-ray, but it has several disadvantages, such as radiation exposure, low resolution-especially in obese patients-and the inability to be reformatted. One advantage of X-ray is its ready availability, especially in peripheral areas, and it can be used as a primary screening modality in the evaluation of back pain. Plain Computed Tomography (CT) scan is useful as an adjunct to MRI in conditions like polytrauma, particularly in the better evaluation of bone fractures with its multiplanar reconstruction. Contrast Enhanced Computed Tomography (CECT) scan, Positron Emission Tomography-Computed Tomography (PET-CT), and nuclear scintigraphy all carry the risk of radiation exposure and require the use of exogenous contrast material/radionuclide injection. Therefore, these imaging modalities cannot be used in pregnant women, paediatric patients, and those with chronic renal disease. The most common conditions causing back pain include degenerative diseases of the spine, benign conditions, inflammatory or infective spondylodiscitis, and benign fractures. Metastasis, primary bone tumours, multiple myeloma, etc., are other spinal diseases that can cause back pain, often accompanied by other symptoms.

Bone marrow is responsible for normal haematopoiesis and accounts for approximately 5% of body weight in an adult human [1,2]. The function of bone marrow is to provide different blood cell lineages involved in tissue nutrition, oxygenation, and the body's immune reactions [3]. The bone marrow mainly contains stem cells responsible for producing erythrocytes, granulocytes, monocytes, lymphocytes, and platelets, and contains supportive cells such as macrophages, adipocytes, osteoblasts, osteoclasts, and adventitial reticular cells, which provide nutrients and cytokines for the proliferation, differentiation, and maturation of haematopoietic cells [2]. These cellular elements are enmeshed within the medullary bony trabeculae, which act as a supporting structure and store calcium and phosphate. There are two types of bone marrow in the spine: red marrow [Table/Fig-1a,b] and yellow marrow [Table/Fig-1c]. The red marrow is named for its richness in haemoglobin in the erythrocyte lineage and is richly vascular, while the yellow marrow, named for its abundant carotenoid bodies in its fat cells, is scarcely vascular [3]. The nutrition of spinal marrow is derived mainly from the ambient sinusoids branching from nutrient vessels piercing the vertebral cortices and drained via Batson's venous plexus. Bone marrow is a dynamic organ with continued changes occurring throughout the life with increased age and increased haematopoietic demands in different health and pathological states [4,5]. These changes in marrow composition contribute to the altered signal characteristics on different MRI sequences. Understanding these signal changes of bone marrow in MRI is key to diagnosing different disease conditions.

Most commonly, marrow signal changes seen in routine MRI are the degenerative end plate changes [Table/Fig-2a-d]. These are classified as Modic type I (oedema), in which the end plate is T1 hypointense and T2 hyperintense, Modic Type II (fatty), in which the end plate is hyperintense on both T1 and T2, and finally Modic type III (sclerosis) [6].

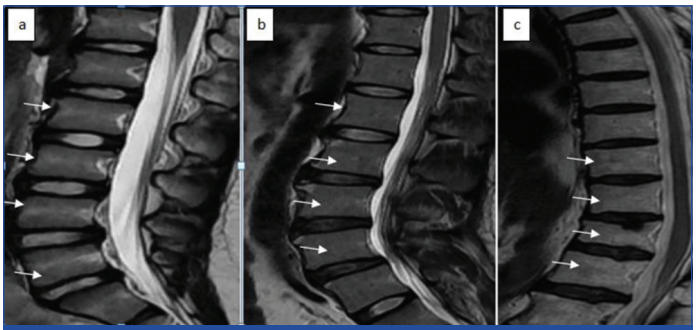

[Table/Fig-1]: Sagittal T2 images: a) Lumbar spine in a 10-year-old boy note the appearance of rich red marrow (arrows); b) The spine of a 27-year-old female note the marrow signal is still red marrow (arrows) and image; c) The spine of a 76-year-old patient note the yellow marrow (arrows) is slightly hyperintense in T2 images compared to image 'a' and 'b'.

CASE SERIES

Case 1

A 39-year-old male patient presented with complaints of a fall from a height one day prior, followed by difficulty in walking and back pain since then. There was no evidence of vomiting, headache,

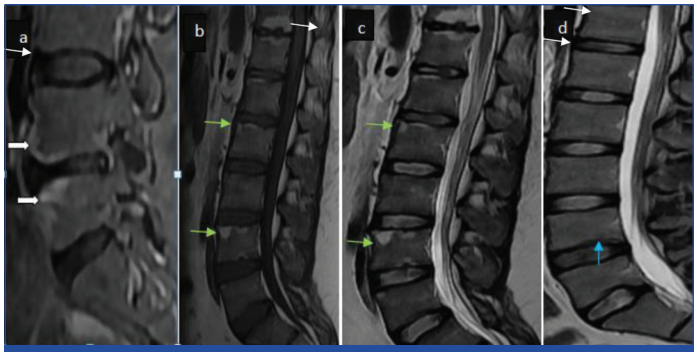

[Table/Fig-2]: Short Tau Inversion Recovery sequence (STIR) sagittal image: a) Modic type 1 (white arrows), sagittal T2 image; b,c) Showing Modic type II (green arrows) and sagittal T2 image; d) Showing subtle end plate hyperintensities suggestive of sclerosis (blue arrow).

or loss of consciousness. Upon general examination, the patient was conscious, coherent, and cooperative, and vitals were stable. Clinical examination revealed paraspinal tenderness noted at the L3-L4 level. The patient was advised MRI lumbar spine screening, which revealed a hypointense horizontal line with subtle marrow oedema involving the L1 vertebra, with a slight decrease in vertebral body height, suggestive of a traumatic compression fracture [Table/Fig-3]. Based on the imaging, the Thoracolumbar Injury Classification and Severity Score (TLICS) [7] was given as one. Consequently, the patient was treated conservatively with rest and analgesic medications.

Below are two companion cases demonstrating the imaging features of benign and insufficiency fractures [Table/Fig-4,5].

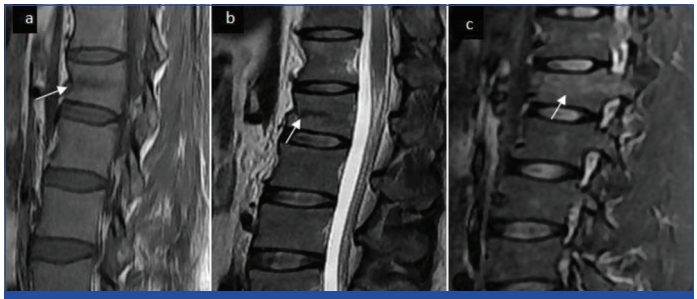

[Table/Fig-3]: Traumatic fracture: T1 sagittal image: a) and Sagittal t2 image; b) Note horizontal hypointense fracture line in L1 vertebra body with marrow oedema in STIR image; c) (arrows) with mild decreased body height.

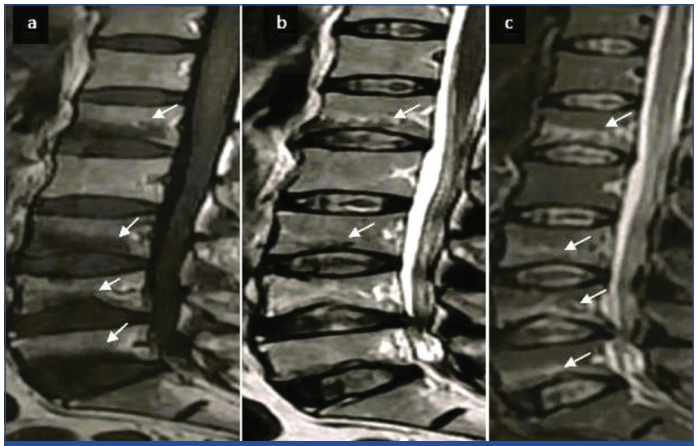

[Table/Fig-4]: Sagittal T1 image; a) Showing end plate hypointensities (arrows); Sagittal T2 b) and Sagittal STIR; c) Showing corresponding end plate hypo intensities in the inferior end plate of multiple lumbar vertebrae (arrows). Note the linear hypointense sub endplate horizontal fracture line parallel to the end plate with associated marrow oedema suggestive of benign end plate insufficiency fractures.

Case 2

A 64-year-old male patient presented with complaints of a sudden fall while walking, followed by weakness of both lower limbs for 15-20 days, along with associated fever, malaise, shortness of breath, and loss of appetite. There was no evidence of bladder or bowel disturbances. Upon general examination, the patient was conscious,

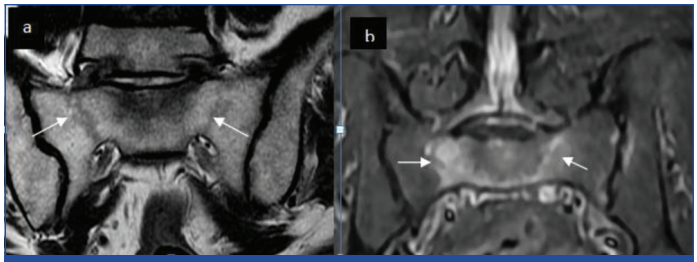

[Table/Fig-5]: Another example of insufficiency fracture involving sacral ala AxialT2 image: a) Showing linear irregular symmetrical fracture lines (arrows) in bilateral sacral ala and coronal STIR image; b) Showing associated bone marrow oedema in sacral ala (arrows).

coherent, and had stable vitals. Neurological examination revealed a decrease in sensation of the left lower limb with a power of 4/5 in both lower limbs. The patient was admitted for further evaluation. Routine blood investigations revealed mild leucopenia, raised Erythrocyte Sedimentation Rate (ESR), and raised C-Reactive Protein (CRP), indicating a suspicion of an infective aetiology. The patient was then referred for an MRI of the dorsal spine, which revealed marrow oedema of the D7 and D8 vertebrae, with thick irregular exudative enhancement seen in the subarachnoid space around the cord at the D7-D8 level, extending into the neural foramina on either side, causing focal bilateral moderate cord compression at this level [Table/Fig-6a-d]. There was cord oedema at the D7-D8 level. Additionally, there was mild enhancement of the subarachnoid space around the cord, extending from D8 to the conus medullaris. Imaging features were suggestive of infective spondylitis, with the possibility of Brucellosis or Tuberculosis, with sparing of the D7-D8 intervertebral disc. Subsequently, a CT-guided biopsy of the D7 vertebra was performed, and the tissue sample was sent for Tuberculosis Polymerase Chain Reaction (TB-PCR) and *Brucella* antibodies, from which the *Brucella* IgG antibody tested positive. The patient was started on tab doxycycline and rifampicin for *Brucella* infection, and the patient showed clinical improvement in the symptoms on follow-up visits.

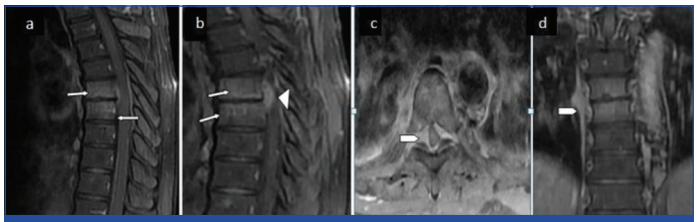

[Table/Fig-6]: Sagittal STIR image a), and sagittal T1 fat sat post-contrast image; b) Showing marrow oedema involving D7 and D8 vertebrae (mainly endplates) with patchy post-contrast enhancement (arrows). Note thick posterior epidural collection at D7-D8 level (Arrowhead). Axial post-contrast image; c) Depicting enhancing collection around the cord (pentagon) causing moderate cord compression at D7-D8 level. Coronal fat sat post-contrast image; d) Depicting small right para vertebral collection (pentagon). Note sparing of D7-D8 disc.

Case 3

A 39-year-old male patient presented with complaints of neck pain, sore throat, fever, and difficulty in swallowing for three months, as well as tingling and numbness in his right upper and lower limbs for the last four days. Upon examination, the patient was conscious, coherent, and cooperative, and his vitals were stable. Clinical examination revealed a bulge and congestion in the pharynx and a few palpable lymph nodes in the neck. The patient was admitted for further evaluation, and all necessary investigations were conducted. Blood investigations showed an elevated Erythrocyte Sedimentation Rate (ESR) and a decrease in lymphocyte count. The patient was advised to undergo an MRI of the cervicodorsal spine, which revealed a large retropharyngeal abscess complicated by a cervical spine epidural abscess, spondylodiscitis, and cervical compressive myelopathy at the C5-C6 level [Table/Fig-7a-d]. The rest of the spine was unremarkable. Imaging features were suggestive of a tubercular aetiology. The retropharyngeal abscess was drained transorally, and the sample was sent for culture and histology. The

culture was positive for tubercular bacilli. The screening chest was unremarkable. The patient was then put on antitubercular therapy for 6-9 months. On follow-up visits, the patient showed clinical improvement.

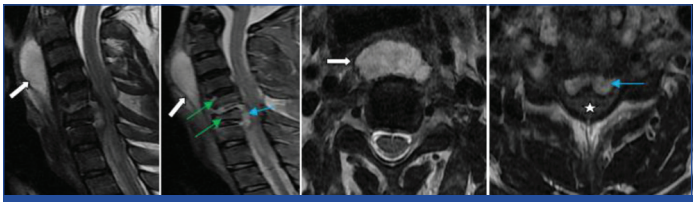

[Table/Fig-7]: Sagittal T2 image a) and STIR image b), Axial T2 image c) and fat-saturated image d) Showing retropharyngeal abscess (white arrows) extending inferiorly along the prevertebral space for a long extent up to D6-D7 level, and extending posteroinferior into the epidural space forming epidural abscess at C6-C7 levels (blue arrows) causing moderate to severe compression of cervical cord (asterisk) at this level- features suggestive of Tubercular retropharyngeal abscess complicated by C6-C7 spondylodiscitis (green arrow) with epidural abscess formation.

Case 4

A 63-year-old male patient presented with complaints of being unable to walk, weakness in both legs, and pain in bilateral lower limbs for 15 days. There was no history of fever, vomiting, or loss of consciousness. The patient had a history of multiple myeloma. Upon general examination, the patient was conscious and coherent, and vitals were stable. Based on previous imaging and other investigations, the patient was diagnosed with multiple myeloma involving the D2-D4 thoracic spine, for which he underwent D2-D4 decompressive laminectomy. On follow-up visits postsurgery, a plain and contrast MRI of the dorsal spine was advised, which showed multilevel heterogeneous patchy and discrete altered marrow signal intensities with variable postcontrast enhancement seen involving almost the entire spine, including the posterior bony elements and bilateral ribs [Table/Fig-8a-d]. The imaging features were suggestive of progression of multiple myeloma. The patient was discharged with a prescription of Tab Pantocid, Tab Linezolid, Tab Enzoheal, Tab Rejyunex Cd3, and 1 Tab Dical-D. On a further one-month follow-up visit, the patient was advised to undergo a repeat follow-up MRI, which revealed newly developed bulky soft-tissue lesions involving the bilateral pedicles and transverse process of the D3 vertebra, suggestive of new onset lesions. At present, the patient is undergoing radiotherapy and chemotherapy.

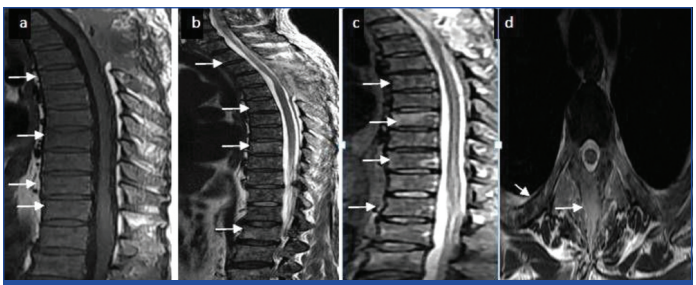

[Table/Fig-8]: Sagittal T1 image a) and sagittal T2 image b) Showing diffuse multilevel patchy and discrete heterogeneous altered marrow Signal Intensity (SI) lesions involving almost entire spine (arrows). Sagittal STIR image c) Showing diffuse heterogeneous marrow oedema and axial T2 image d) Note involvement of spinous process of D12 vertebra including ribs (arrow).

Case 5

A 30-year-old male patient presented with complaints of lower backache for 25 days, which he experienced while riding a bike, as well as swelling on the left-side of the neck. Upon general examination, the patient was conscious and coherent, and his vitals were stable. Clinical examination revealed tenderness in the paraspinal muscles, with no evidence of focal neurological deficits. The patient was admitted for primary evaluation and supportive management, and all necessary investigations were conducted. The MRI of the dorsal spine revealed multilevel ill-defined lesions with patchy marrow oedema in the dorsal vertebrae, along with an anterior wedge compression fracture of the D11 vertebra (resulting in a 50-60% decreased body height) [Table/Fig-9a-d]. In addition, the posterior bony elements of the D5, D9, and D11 vertebrae were also involved. A few enlarged para-aortic lymph nodes were also noted in the scan. Based on these findings, the diagnosis of spinal metastasis was made. To determine the primary site, a PET-CT scan was performed, which revealed multiple bony and liver metastases, with a suspected primary site in the stomach. An endoscopy-guided biopsy from the stomach confirmed adenocarcinoma of the stomach. Fine Needle Aspiration Cytology (FNAC) of the supraclavicular lymph nodal swelling revealed adenocarcinoma metastasis. Emergency radiation to the dorsal spine was advised, but the patient refused, and he was discharged with a prescription of Tab dexamethasone 8 mg (1 tablet BD), Tab morphine plain 10 mg (1 tablet 6 times daily), Tab gabanet at bedtime, and Tab ondansetron 8 mg (1 tablet BD). On follow-up, the patient succumbed to the disease within one month.

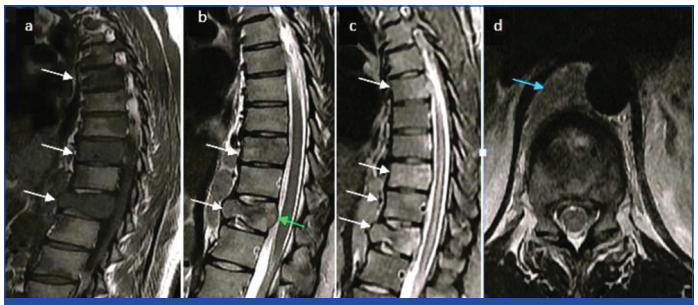

[Table/Fig-9]: Sagittal T1 image a), Sagittal T2 image b), and Sagittal STIR image c) Depicting multilevel ill-defined lesions with patchy marrow oedema seen in the thoracic vertebrae (white arrows) with reduced anterior body height of D11 vertebra (50-60% decreased body height). The convex bulging of posterior cortex of D11 (green arrow). There is mild spinal canal compression at D11 level (AP canal dimension 10 mm). Features were s/o vertebral metastasis. Enlarged para-aortic metastatic lymph node in Image d (blue arrow).

Case 6

A 40-year-old female patient presented with a chronic history of easy fatigue, back pain, decreased appetite, and weight loss for 7-8 months. On physical examination, she exhibited severe pallor, mild glossitis, and a bounding pulse with borderline blood pressure of 160/90. She was advised to undergo routine blood investigations and an MRI of the lumbar spine to evaluate her back pain. The lab reports revealed a low haemoglobin level of 6 g/dL and mild vitamin B12 deficiency. The cause of her anaemia was found to be nutritional anaemia. The MRI of the lumbar spine revealed haematopoietic marrow hyperplasia due to chronic severe anaemia [Table/Fig-10a,b], with no evidence of significant disc bulges or nerve root compression noted on the MRI scan. She was prescribed

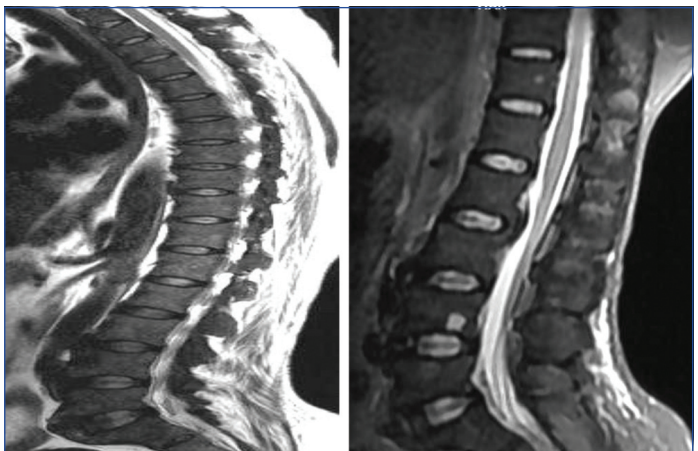

[Table/Fig-10]: Sagittal T2 image a) and Sagittal STIR image b) Note diffuse low marrow Signal Intensity (SI) of entire spine in a case of chronic anaemia– s/o haematopoietic hyperplasia of red marrow.

vitamin B12 and iron tablet supplements and advised to follow a proper nutritional diet. On follow-up, the patient's symptoms had improved.

DISCUSSION

The abnormal marrow in the spine can exhibit different patterns and signal characteristics. This article mainly focuses on describing these various pathological marrow conditions in different clinical contexts, thereby helping to narrow the differential diagnosis. Routinely, MRI T1, T2 weighted, and fat suppression sequences were used to assess the marrow abnormalities. Diffusion Weighted Image (DWI) is useful in differentiating osteoporotic versus neoplastic vertebral fractures [8], in differentiating infective versus degenerative endplate changes [9], and in the follow-up of neoplastic vertebral lesions [10]. The role of DWI is controversial in studying the bone marrow, and however, it should be interpreted in line with other native sequences [11,12].

The very common signal changes that radiologists observe on routine MRI spine images include red marrow, which is highly vascular, yellow marrow, which is fatty, fatty nodular hyperplasia, islands of red marrow hyperplasia, haemangiomas, enostosis, and so on. [Table/Fig-11] briefly describes the signal characteristics of these different conditions on different MRI sequences.

T1	T2	STIR/fat saturated sequence	Conditions
Low	Low	Low	Diffuse osteosclerosis, as in renal osteodystrophy, radiation-induced
High	High	May or may not suppresses	Hemangiomas (stippled appearance)/ focal fatty nodules
Low	Slightly hyper	Hyper	Represent marrow oedema as in infections, inflammatory, metastasis benign/ malignant fractures
Low (not lower than adjacent disc)	High	Slightly hyper/ Intermediate	Red marrow as in young age, haematopoietic marrow hyperplasia as in chronic anaemia
High	High	Signal suppressed	Yellow marrow as in old age or radiation-induced changes
Heterogeneous	Heterogeneous	Heterogeneous	Diffuse diseases as in multiple myeloma, leukaemic infiltrates

[Table/Fig-11]: Describes the common marrow signal changes seen on routine practice.

Marrow signal alterations can be diffuse, involving most or the entire spine, as in multiple myeloma, myelofibrosis, marrow reconversion states as in chronic anaemia, leukaemia, and metabolic diseases, or focal, limited to one vertebra or one vertebral segment, as in the case of solitary metastasis, infective spondylodiscitis, primary vertebral tumours like giant cell tumour.

Haematopoietic red marrow hyperplasia can pose a diagnostic dilemma sometimes, but most often the Signal Intensity (SI) on T1 is not lower than the adjacent disc/muscle.

One of the most commonly seen lesions on routine MRI spine are haemangiomas. Typical haemangiomas are bright on T1 and T2W images [Table/Fig-12], and on STIR images, they may show signal suppression or sometimes show high-SI on STIR due to slow flow in vascular channels [13]. Its benign nature is ascertained by corresponding high-SI on T1W images due to its abundant fat content. Metastases show cortical destruction more often than haematopoietic malignancies [14].

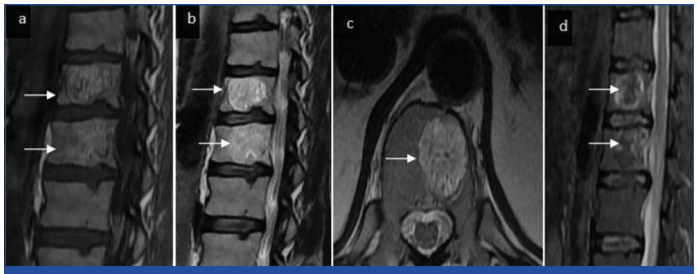

[Table/Fig-12]: T2 image a-d) Showing T1 and T2 hyperintense lesions in D12 and L1 vertebral bodies with variable suppression on STIR image. Note the stippled appearance on the axial image (c) Suggestive of haemangioma.

Traumatic or Benign Fractures

Traumatic fractures are usually wedge compression fractures or burst fractures with marrow oedema in the case of acute trauma, or associated cord injury depending on the type and severity of the fracture, with or without paraspinal haemorrhage or collection. On MRI, benign fractures from malignant fractures can be readily differentiated based on the fact that benign fractures will have a low SI fracture line that is parallel to vertebral end plates. On the other hand, malignant fractures show diffuse vertebral body marrow oedema, convex bulging of the posterior cortex, an absent fracture line, marrow oedema involving pedicles, with or without an associated paraspinal soft-tissue component [15].

Tuberculosis of Spine

One of the most common infections of the spine in India is tubercular spondylodiscitis. There are three main patterns of spine involvement in tuberculosis: paradiskal, anterior, and central [16]. Jung NY et al., found that MRI showed a sensitivity of 100%, a specificity of 80%, and an accuracy of 90% in diagnosing TB when compared to pyogenic infection [17]. Their most indicative signs of vertebral TB were: well-defined paraspinal abnormal signal, thin and smooth abscess wall, combination of both findings, presence of soft-tissue or intraosseous abscess, subligamentous spread to three or more vertebral levels, involvement of multiple vertebral bodies, thoracic spine localisation.

Brucellosis of Spine

Brucellosis needs to be differentiated from tuberculosis because both require different management and have different prognoses. Commonly, brucellosis involves vertebral end plates, adjacent vertebrae, with minor bone destruction [18], sparing vertebral morphology. It usually doesn't affect the posterior elements, and paravertebral or psoas abscesses are rare. Additionally, disc spaces are spared early in the disease. In present case, most of these features described for spinal brucellosis were present, making it a classical case of brucellosis.

Multiple Myeloma

There are five different types of marrow signal changes described in multiple myeloma. The first type is that of normal marrow. The second pattern is focal infiltration, which appears as focal hypointense on T1, and focal hyperintense on T2/STIR images. The third pattern is diffuse bone marrow infiltration, which appears as a homogeneous hypointense T1 signal, and a homogeneous hyperintense T2/STIR signal. The fourth pattern is combined focal and diffuse infiltration, which appears as a diffuse hypointense T1 signal, interspersed with focal hyperintense T2/STIR lesions. The last pattern is the typical "salt-and-pepper" infiltration, which appears as patchy, inhomogeneous T1 and T2 signal [19]. In present case of multiple myeloma, the fourth pattern was observed, which is focal and diffuse. [Table/Fig-13] briefs the different patterns of spinal marrow changes in different pathological conditions and helps narrow the differentials.

Focal involvement of spine	
T1 hyper T2 hyper STIR suppression	Haemangiomas
End plate linear parallel hypointense bands with preserved normal marrow [20].	Benign end palate insufficiency fracture
Within the fractured vertebral body if a marrow signal is lost	Pathological fracture
Multiple levels (more than two vertebral segments) Marrow oedema with or without adjacent disc involvement with paravertebral abscess with smooth enhancing m wall	Tubercular spondylodiscitis
The abscess wall is irregular and less than 2 vertebral segments	Pyogenic or non tubercular spondylodiscitis
If the spine is diffusely involved	
Convex bulging of the posterior cortex and Posterior elements involved	Spine metastasis
Diffuse heterogeneous multilevel marrow signal changes	Multiple myeloma and also low ADC than metastasis [21]
Diffuse low signal intensities	Haematopoietic marrow hyperplasia as in metabolic disease or chronic anaemia

[Table/Fig-13]: Briefing different pattern-based differentiation of different diseases of the spine [20,21].

CONCLUSION(S)

The MRI spine is the most preferred imaging modality for the evaluation of back pain, which is the most common presenting symptom in most spinal pathologies. Knowledge of marrow signal alterations on MRI in different age groups and different disease conditions is very important for differentiating normal marrow from abnormal and further distinguishing among abnormal pathological conditions. This article describes the appearance of normal marrow signal changes on different MRI sequences with age and details the salient features of different pathological conditions.

REFERENCES

[1] Vogler 3rd JB, Murphy WA. Bone marrow imaging. Radiology. 1988;168(3):679-93.
[2] Travlos GS. Normal structure, function, and histology of the bone marrow. Toxicologic Pathology. 2006;34(5):548-65.
[3] Riley RS, Williams D, Ross M, Zhao S, Chesney A, Clark BD, et al. Bone marrow aspirate and biopsy: A pathologist's perspective. II. interpretation of the bone marrow aspirate and biopsy. J Clin Lab Anal. 2009;23(5):259-307.
[4] Strong PN, Goerke J, Oberg SG, Kelly RB. Beta-Bungarotoxin, a pre-synaptic toxin with enzymatic activity. Proceedings of the National Academy of Sciences. 1976;73(1):178-82.
[5] Vande Berg BC, Malghem J, Lecouvet FE, Maldague B. Magnetic resonance imaging of the normal bone marrow. Skeletal RADIOLOGY. 1998;27:471-83.
[6] Modic MT, Steinberg PM, Ross JS, Masaryk TJ, Carter JR. Degenerative disk disease: Assessment of changes in vertebral body marrow with MR imaging. Radiology. 1988;166(1):193-99.
[7] Vaccaro AR, Lehman Jr RA, Hurlbert RJ, Anderson PA, Harris M, Hedlund R, et al. A new classification of thoracolumbar injuries: The importance of injury morphology, the integrity of the posterior ligamentous complex, and neurologic status. Spine. 2005;30(20):2325-33.
[8] Karchevsky M, Babb JS, Schweitzer ME. Can diffusion-weighted imaging be used to differentiate benign from pathologic fractures? A meta-analysis. Skeletal radiology. 2008;37:791-95.
[9] Eguchi Y, Ohtori S, Yamashita M, Yamauchi K, Suzuki M, Orita S, et al. Diffusion magnetic resonance imaging to differentiate degenerative from infectious endplate abnormalities in the lumbar spine. Spine. 2011;36(3):E198-202.
[10] Padhani AR, Koh DM, Collins DJ. Whole-body diffusion-weighted MR imaging in cancer: Current status and research directions. Radiology. 2011;261(3):700-18.
[11] Baur A, Huber A, Dürr HR, Nikolaou K, Stäbler A, Deimling M, et al. Differentiation of benign osteoporotic and neoplastic vertebral compression fractures with a diffusion-weighted, steady-state free precession sequence. RoFo: Fortschritte auf dem Gebiete der Rontgenstrahlen und der Nuklearmedizin. 2002;174(1):70-75.
[12] Castillo M, Arbelaez A, Smith JK, Fisher LL. Diffusion-weighted MR imaging offers no advantage over routine noncontrast MR imaging in the detection of vertebral metastases. Am J Neuroradiol. 2000;21(5):948-53.
[13] Baudrez V, Galant C, Vande Berg BC. Benign vertebral hemangioma: MR-histological correlation. Skeletal Radiology. 2001;30:442-46.
[14] Parfitt AM. The hyperparathyroidism of chronic renal failure: A disorder of growth. Kidney International. 1997;52(1):03-09.
[15] Jung HS, Jee WH, McCauley TR, Ha KY, Choi KH. Discrimination of metastatic from acute osteoporotic compression spinal fractures with MR imaging. Radiographics. 2003;23(1):179-87.
[16] Weinstein SL. The Pediatric spine principles and practice. Lippincott Williams & Wilkins; 2001.
[17] Jung NY, Jee WH, Ha KY, Park CK, Byun JY. Discrimination of tuberculous spondylitis from pyogenic spondylitis on MRI. Am J Roentgenol. 2004;182(6):1405-10.
[18] Erdem H, Elaldi N, Batirel A, Aliyu S, Sengoz G, Pehlivanoglu F, et al. Comparison of brucellar and tuberculous spondylodiscitis patients: Results of the multicenter "Backbone-1 Study". The Spine Journal. 2015;15(12):2509-17.
[19] Dutoit JC, Verstraete KL. Whole-body MRI, dynamic contrast-enhanced MRI, and diffusion-weighted imaging for the staging of multiple myeloma. Skeletal Radiology. 2017;46:733-50.
[20] Yuh WT, Zachar CK, Barloon TJ, Sato Y, Sickels WJ, Hawes DR. Vertebral compression fractures: Distinction between benign and malignant causes with MR imaging. Radiology. 1989;172(1):215-18.
[21] Park GE, Jee WH, Lee SY, Sung JK, Jung JY, Grimm R, et al. Differentiation of multiple myeloma and metastases: Use of axial diffusion-weighted MR imaging in addition to standard MR imaging at 3T. PLoS One. 2018;13(12):e0208860.

PARTICULARS OF CONTRIBUTORS:
1. Assistant Professor, Department of Radiology, Malla Reddy Medical College for Women, Hyderabad, Telangana, India.
2. Associate Professor, Department of Orthopaedics, Subbaiah Institute of Medical Sciences, Shimoga, Karnataka, India.
3. Assistant Professor, Department of Radiology, Malla Reddy Medical College for Women, Hyderabad, Telangana, India.
4. Junior Resident, Department of Radiology, Malla Reddy Medical College for Women, Hyderabad, Telangana, India.
5. Professor, Department of Radiology, Malla Reddy Medical College for Women, Hyderabad, Telangana, India.

NAME, ADDRESS, E-MAIL ID OF THE CORRESPONDING AUTHOR:
Dr. Sree Sreya Chinnapolla,
Junior Resident, Department of Radiology, Malla Reddy Medical College for Women, Hyderabad-500055, Telangana, India.
E-mail: sreyachowdary96@gmail.com

PLAGIARISM CHECKING METHODS: [Jain H et al.]
- Plagiarism X-checker: Nov 11, 2023
- Manual Googling: Dec 19, 2023
- iThenticate Software: Dec 20, 2023 (8%)

ETYMOLOGY: Author Origin

EMENDATIONS: 5

AUTHOR DECLARATION:
- Financial or Other Competing Interests: None
- Was informed consent obtained from the subjects involved in the study? No
- For any images presented appropriate consent has been obtained from the subjects. No

Date of Submission: **Nov 08, 2023**
Date of Peer Review: **Dec 08, 2023**
Date of Acceptance: **Dec 20, 2023**
Date of Publishing: **Jan 01, 2024**